ACS APPLIED MATERIALS & INTERFACES

RESEARCH ARTICLE

www.acsami.org

# nPEG-$TiO_2$ Nanoparticles: A Facile Route to Elaborate Nanostructured Surfaces for Biological Applications

J. Spadavecchia, S. Boujday, J. Landoulsi, and C.-M. Pradier*

Laboratoire de Réactivité de Surface, Université Pierre et Marie Curie-Paris 06, CNRS UMR 7197, 4 Place Jussieu, Case 178, F-75005 Paris, France

**ABSTRACT:** We report the synthesis of diacid-terminated PEG-functionalized cubic $TiO_2$ nanocrystals by a simple one-step solvothermal method, and their further use to form nanostructured surfaces for protein immobilization. The relevance and major interest of the so-obtained nanocrystals are the presence of terminal carboxylic acid groups at their surface, as confirmed by infrared analyses, in addition to the surrounding PEG chains, essential to avoid non specific interactions. These functional chemical groups were used to (i) immobilize the synthesized nanocubes on a cysteamine-modified Au surface, and to (ii) attach proteins via a presumable covalent link. AFM images show that the shapes and the narrow size distribution of the nanocubes, observed by TEM, were preserved after their immobilization on the modified Au surface. Moreover, the efficiency and specificity of antigen recognition were demonstrated using spectroscopic analyses. Our successful approach provides a versatile and facile way to elaborate specific and sensitive nanostructured surfaces for biosensors.

**KEYWORDS:** $TiO_2$ nanoparticles, nanostructured surface, TEM, IR, AFM, biosensor

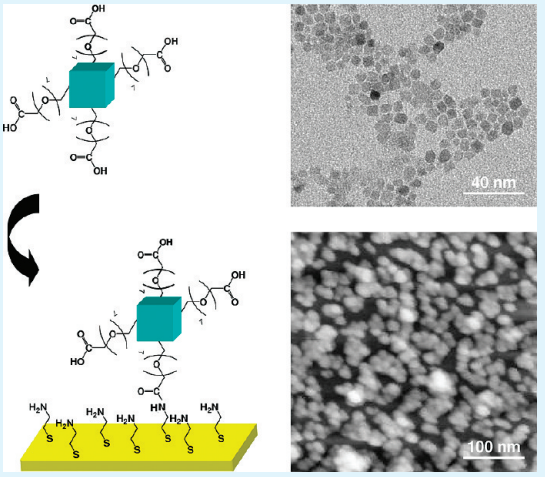


$TiO_2$ nanoparticles (NPs) have become a modern and widely used material in nanotechnologies because of their unique and tunable size-dependent electrical, magnetic, optical and chemical properties, which largely differ from those of bulk titanium oxide.[1−3] $TiO_2$ NPs have been applied to the preparation of biomaterials and biosensors owing to their biocompatibility, stability and strong adsorptive ability on various electrode materials.[4,5] Some authors have utilized $TiO_2$ NPs to immobilize heme proteins and develop biosensors for nitric oxide and carbon oxide detection.[6,7] Other authors have elaborated hydrogen peroxide biosensors based on the immobilization of peroxidases, thanks to the possible direct electron transfer between the enzymes and $TiO_2$ NPs.[8] Studies on $TiO_2$ nanocrystals have mostly been focused on controlling structural and morphological properties without taking advantage of their surface chemical functionalities. These features may govern interfacial processes involved in various applications with biologic interest. Several methods can be used to elaborate $TiO_2$ NPs with a high crystallinity and controlled shape and size. These well known procedures often necessitate supercritical drying[9] or high-temperature calcination.[10] In these methods, the use of surfactants enables the synthesis of crystalline and well-dispersed NPs, but these compounds are often toxic, expensive, and require relatively high temperatures for their decomposition.[11] An alternative route is the use of solvothermal methods to elaborate $TiO_2$ NPs[12] starting from an alkoxide precursor (titanium isopropoxide, Ti(OPri)$_4$) and a carboxylic function like acetic acid (AA). The introduction of acetic acid in the synthesis process is known to better control the hydrolysis and condensation rates by gradually introducing water into the system. Acetic acid is also able to confine the crystal growth.[13] Moreover, modulating the Ti(OPri)$_4$/AA ratio and temperature allows the elaboration of $TiO_2$ NPs with tunable shapes and sizes.[12]

NPs may have a huge potential for the elaboration of nanostructured surfaces, when immobilized on flat surfaces, to be used in biological applications. For this purpose, two features are of major importance: (i) the presence of chemical groups on the NPs surface, required for both their immobilization and the attachment of (bio)macromolecules, and (ii) the control of NPs dispersion as they often display an extremely high tendency to adhesion and aggregation,[14] because of their multiple surface structures.

The aim of this work is to develop a one step-procedure to synthesize $TiO_2$ NPs that expose chemical groups in view of creating functional and highly ordered surfaces. Dicarboxylic poly(ethylene glycol) (PEG) was chosen to guarantee non fouling characteristics, while ensuring a satisfying accessibility of immobilized proteins for bio-recognition. The shape of $TiO_2$ NPs, depending on the chemical structure and conformation of the PEG chains, may influence the orientation of proteins grafted on these nanostructured surfaces. Moreover, the presence of

**Received:** April 11, 2011
**Accepted:** June 6, 2011
**Published:** June 06, 2011

**Scheme 1. Proposed Formation Mechanism of nPEG-$TiO_2$ NPs in Dicarboxylic Acid-Termninated PEG and Benzyl Alcohol**

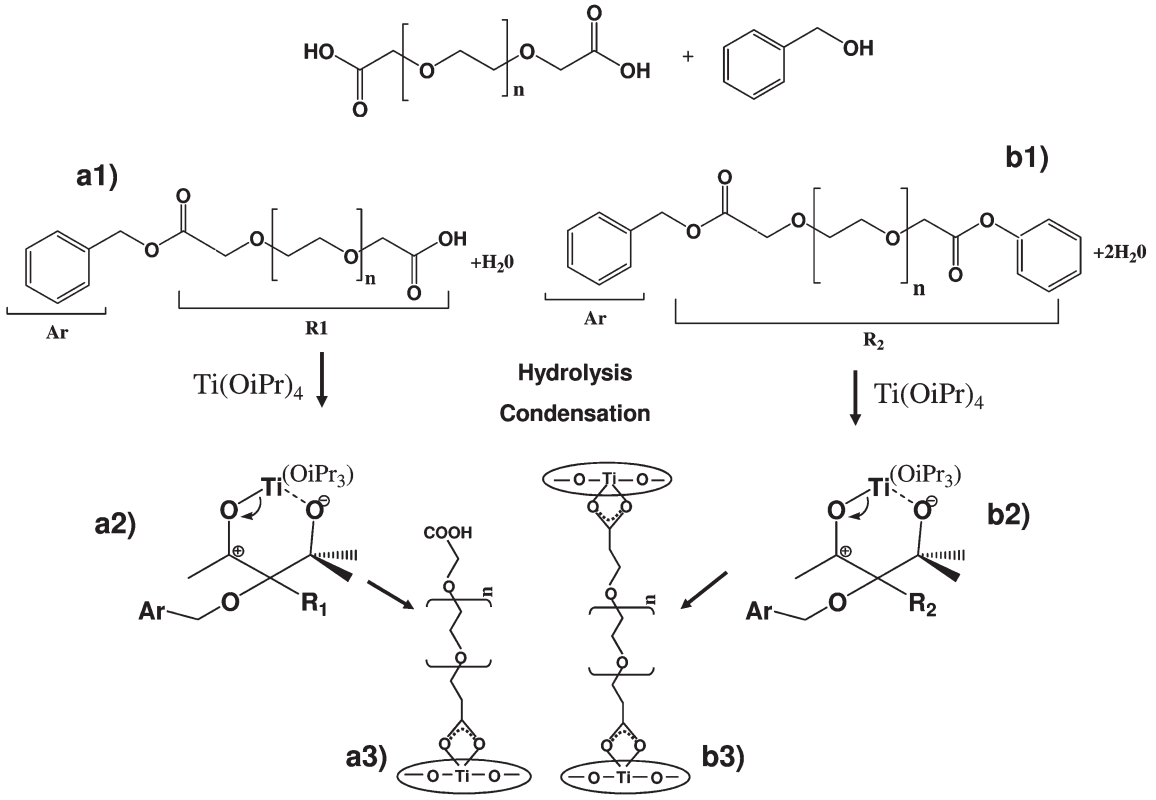


end-tethered PEG at solid interfaces is expected to impede nonspecific protein adsorption.[15]

## EXPERIMENTAL SECTION

**Materials.** Ti(IV) isopropoxide ($Ti(OPri)_4$, 97%), benzyl alcohol (BzOH, ≥99%), polyethylene glycol 600 Diacid (PEG-diacid; $M_w$ = 600 Da), cysteamine, *N*-hydroxysuccinimide (NHS), 1-(3-dimethylaminopropyl)-*N*′-ethylcarbodiimide hydrochloride (EDC), dimethylformamide for molecule biology (DMF, 99%), buffer solution ($K^+$ phthalate, pH 9), were purchased from Sigma Aldrich (Saint-Quentin Fallavier, France). All solvents were reagent-grade and used without any further purification. Rabbit IgG (rIgG) and bovine serum albumin (BSA) were purchased from Sigma-Aldrich (France). The monoclonal mouse antibody against the Fc fragment of rabbit IgG (anti-rIgG), was provided by ENSAR/INRA (Agrocampus-Rennes, Département des sciences animales, France). Experiments were carried out at room temperature if not specified otherwise. For surface analyses, glass substrates (11×11 $mm^2$), successively coated with a 5 m, thick layer of chromium and a 200 nm thick layer of gold, were purchased from Arrandee (Werther, Germany). The gold-coated substrates were annealed in a butane flame to ensure a good crystallinity of the topmost layers and rinsed in a bath of absolute ethanol for 15 min before use.

**$TiO_2$ NPs Synthesis.** $TiO_2$ NPs were prepared according to the following procedure: 1 mL portion of $Ti(OPri)_4$ (3.36 mmol) was added to 0.75 mL of PEG-diacid and 5 mL of BzOH ($Ti(OPri)_4$/ PEG-diacid 1/5). The solution was stirred for 30 min at room temperature after which the mixture were transferred into a steel autoclave equipped with a Teflon cap and kept to 200 °C for 18 h; during this time the solution turns from clear to yellow milky suspension. The reaction was then stopped and the suspension was centrifuged two times (9000 rpm for 30 min). The white precipitate became slightly yellow upon washing with ethanol and dichloromethane twice; it was then dried in a vacuum.

**Immobilization Procedures.** Chemistry procedures based on SAMs of cysteamine in absolute ethanol have been described previously.[21] Briefly, the freshly cleaned gold substrate was immersed in an unstirred 10 mM ethanol solution of β-mercaptoethylamine (cysteamine) at room temperature, in the dark, for 6 h. The gold substrate was then washed with ethanol and ultapure water (Milli-Q, Millipore, France) to remove the excess of thiols.

For nPEG-$TiO_2$ immobilization on Cysteamine-functionalized gold substrates, 20 mg of nPEG-$TiO_2$ was dissolved in 5 mL of DMF and then 0.5 equiv. of EDC/NHS was added and stirred for 2h (pre-activation). The milky homogeneous suspension was deposited onto cysteamine modified-gold substrates for 12h at room temperature. After rinsing in DMF and ethanol, the substrates were treated with a solution of NHS/EDC in water for 4 h (activation) and then immersed in a buffered solution of proteins (Anti-IgG, BSA, r-IgG) (pH 9).

For PM-IRRAS analyses, anti-rIgG (50 mg/L in buffer solution) was deposited on the PEG-$TiO_2$ NPs surface. After 1h, the surface was rinsed in buffer solution then Milli-Q water for 10 min. A BSA solution (50 mg/L, buffer pH 9) was then used to check the non specific protein adsorption and block the potential residual reactive sites. After 20 min BSA solution was removed by washing with buffer, Milli-Q water, and dried under nitrogen. Specific antigen interaction was then evaluated using a buffer solution containing rIgG (50 mg/L) during 1 h followed by rinsing and drying with the same procedure.

**Powder and Surface Characterizations.** For IR analyses in ATR (attenuated total reflection) mode, $TiO_2$ powder was deposited on an ATR Ge crystal. IR spectra were recorded using a Nicolet 5700 FT-IR spectrometer by recording 256 scans at 8 $cm^{-1}$ resolution. The spectrometer is equipped with a liquid-nitrogen-cooled MCT detector.

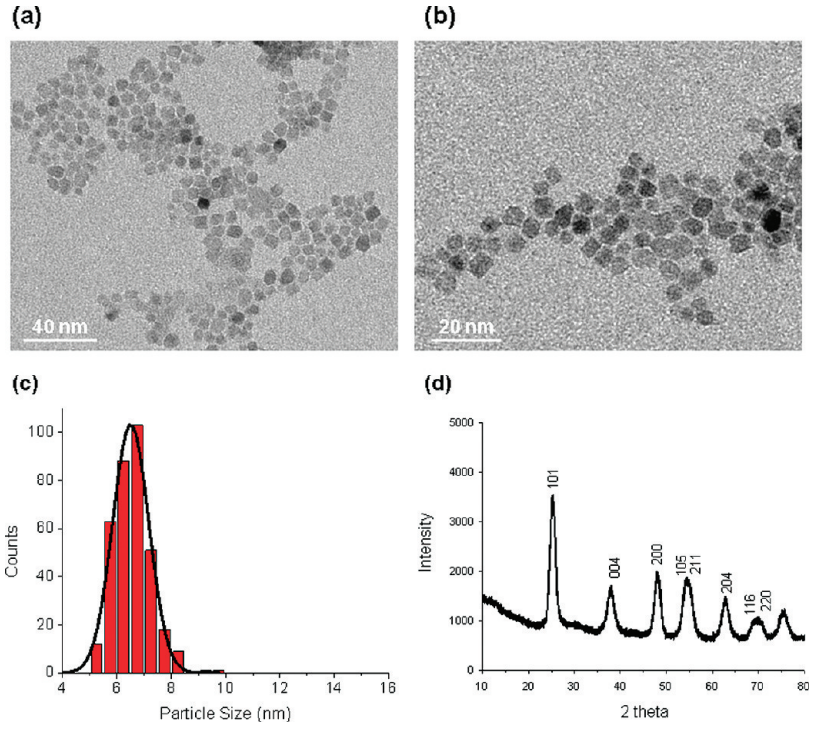


**Figure 1.** Structural analysis of nPEG-$TiO_2$: (a, b) TEM images, (c) particle size distribution, (d) XRD pattern.

PM-IRRAS spectra were recorded on a commercial Thermo-scientific (France) Nexus spectrometer. The external beam was focused on the sample with a mirror, at an optimal incident angle of 80°. A ZnSe grid polarizer and a ZnSe photoelastic modulator, modulating the incident beam between *p*- and *s*-polarizations (HINDS Instruments, PEM 90, modulation frequency = 37 kHz), were placed prior to the sample. The light reflected at the sample was then focused onto a nitrogen-cooled MCT detector. The presented spectra result from the sum of 128 scans recorded with 8 $cm^{-1}$ resolution.

AFM images were recorded in Peak Force Tapping mode, newly developed (Bruker Nano Inc.-Nano Surfaces Division, Santa Barbara, CA). In this mode, the z-piezo, modulated far below the cantilever resonance frequency, performs very fast approach-retracting curves at each pixel of the image. The peak interaction forces obtained is thus used as the imaging feedback signal, allowing the applied force to be lower than in normal tapping mode. Oxide-sharpened microfabricated $Si_3N_4$ cantilevers (Bruker Nano Inc.-Nano Surfaces Division, Santa Barbara, CA) with a spring constant of 0.36 N/m (as verified with the thermal noise method) and a curvature radius of ~10 nm (manufacturer specified), were used at a scan rate of 1−2 Hz. Images were obtained at room temperature (20−22 °C) in air. All images shown in this paper are flattened raw data.

## RESULTS AND D ISCUSSION

In this study, the synthesis of NPs was performed in a reactive solvent containing titanium isopropoxide and benzyl alcohol, in which dicarboxylic acid-terminated PEG was added. Water production results from the simple or double esterification reactions (Scheme 1) between benzyl alcohol and one (Scheme 1, Reaction a1) or two (Scheme 1, reaction b1) acid functions of PEG-diacid. $Ti(OiPr)_4$ then undergoes several hydrolysis condensation reactions to form $TiO_2$ particles (Scheme 1, reactions a2 and b2). PEG diacid can also act as ligand. Two mechanisms of adsorption may occur: a simple adsorption, leaving one acid terminal function (Scheme 1, reaction a3) or, a double adsorption where PEG acts as a chelating ligand (Scheme 1, reaction b3). The adsorption of PEG on the surface of $TiO_2$ NPs leads to the formation of a monodisperse phase due to steric effects and interparticle repulsion.

Regarding the morphology of the PEGylated nanocrystals, TEM images reveal separated and well-defined NPs with an original cubic shape (Figure 1a and b). TEM images also show that NPs present a good dispersion with no tendency to aggregation (Figure 1a), in contrast to results obtained in many previous studies.[16−19] On the basis of several TEM images, it is clearly shown that NPs have a narrow size distribution (6.6 ± 0.5 nm, Figure 1c). The low aggregation level observed may be due to the repulsive interactions between PEG-chains present at the surfaces of NPs. More direct evidence of the NPs crystallinity is given by XRD analysis performed on the nPEG-$TiO_2$ powder (Figure 1d). The X-ray diffraction spectrum, compared with the well-known standard anatase pattern,[20] indicates the presence of NPs in anatase form, highly crystalline, and without structural defects. Furthermore, results show broad diffraction peaks, characteristic of very small crystallites of about 7.0 nm calculated from the (101) reflection using Scherrer's equation.[11] The particle size determined by XRD is in a good agreement with that obtained by TEM (Figure 1c).

The powder of nPEG-$TiO_2$ NPs was also characterized by IR spectroscopy in ATR mode to check the presence of organic ligands and terminal COOH groups. The resulting spectrum is shown in Figure 2 (Panel A). A large band at 1725 $cm^{-1}$ due to the $\upsilon C{=}O$ stretching mode of the carboxylic groups is observed. This band is broad, with a shoulder towards lower wavenumbers, owing to the contribution of water molecules (still visible in IR-ATR spectrum). The $\upsilon C{-}O$ symmetric stretching mode of the carboxylate groups is present at 1415 $cm^{-1}$. The spectrum also

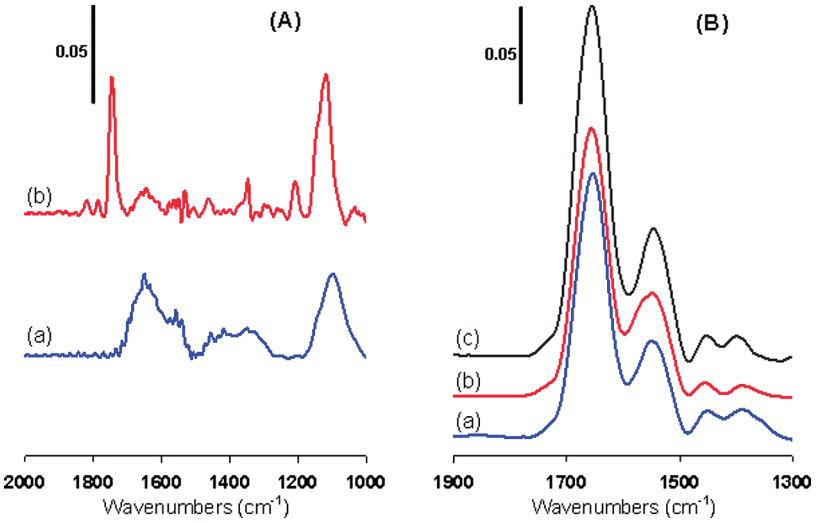


**Figure 2.** Panel A (a) IR-ATR analyses of nPEG-$TiO_2$ powder, (b) PM-RAIRS spectrum of immobilized nPEG-$TiO_2$ on a cysteamine terminated gold surface. Panel B PM-RAIRS spectra obtained on immobilized nPEG-$TiO_2$ after adsorption of (a) anti-rIgG, (b) anti-rIgG +BSA, and (c) anti-rIgG +BSA +rIgG.

**Scheme 2. Schematic Representation of the Biosensor Elaboration Strategy: (a) Au Surface Modification with Cysteamine Self-Assembled Monolayer, (b) nPEG-$TiO_2$ Immobilization via Amide Bond Formed between Activated COOH Groups (using EDC/NHS) Originating from NPs and Amine Group of Cysteamine, (c) Second Activation of nPEG-$TiO_2$ and Binding of Antigens and Antibody Recognition**

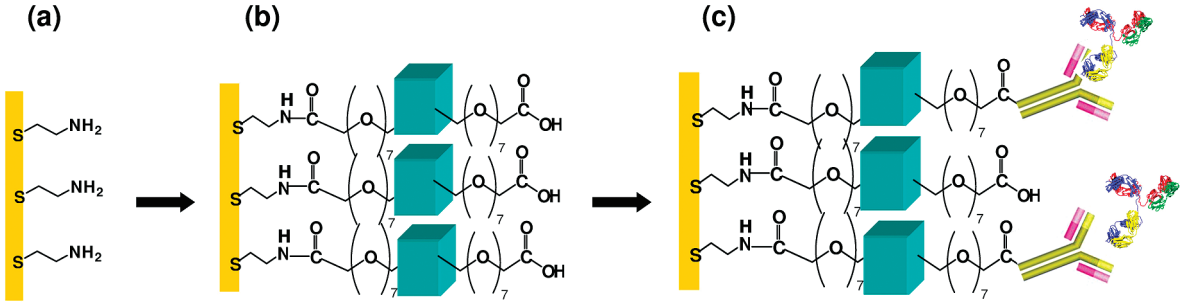


shows the characteristic vibration band of the PEG chain (C−O−C) at 1100 $cm^{-1}$. All these features are in agreement with the presence of PEG-diacid ligands on $TiO_2$ NPs.

The synthesized NPs were used as a support for protein immobilization in view of investigating specific protein−protein interactions for biosensing applications. Prior to protein adsorption, NPs were immobilized on a chemically modified Au surface, as depicted in Scheme 2. To this end, nPEG-$TiO_2$ NPs were preactivated in a solution of EDC/NHS during 2 h at room temperature (preactivaction step). Then, the milky homogeneous suspension of NPs was added to a cysteamine-modified gold surface[21] for 12 h at room temperature to form an amide link between a COOH group originating from nPEG-$TiO_2$ NPs and $NH_2$ end groups of the cysteamine gold surface. After rinsing in DMF and EtOH, the gold substrates were treated again by the solution of NHS/EDC in water for 4 h (activation step). This procedure aims at forming an amide link between a second COOH end-group of nPEG-$TiO_2$ NPs and $NH_2$ groups of protein (Anti-rIgG) deposited on the activated nPEG-$TiO_2$ NPs surface. Surface organization was investigated using atomic force microscopy (AFM). Images were recorded on dried samples using Peak Force Tapping mode. AFM images revealed the presence of well-defined NPs, highly dispersed on the gold surface. The NPs are either isolated or close to each other, but only few aggregates can be observed (Figure 3a, b). The NPs density, evaluated from a statistical analysis of 1 × 1 $\mu m^2$ image, is on an average close to 1.4 × $10^{14}$ NPs per square centimeter. Regarding the NPs size, cross-sections indicated that the particles are homogenous (particle height near 7 nm, Figure 3c). When the particles were in close contact with each other, the AFM tip was too large to go into the interstices between particles. However, cross section revealed that the particle height is almost the same when NPs are isolated or in close contact (Figure 3c). Accordingly, a height size distribution was made on the basis of a total of about 100 cross sections performed along the 1 × 1 $\mu m^2$ image. Results given in Figure 3d show a NPs size of 6.7 nm ±0.8 nm in diameter, in agreement with observations made with TEM and XRD on $TiO_2$ NPs powder. These findings indicate that $TiO_2$ NPs, when immobilized on functionalized gold surface, presumably via covalent link, preserve their size and shape. The narrow size distribution suggests that NPs are randomly immobilized on the gold surface and validate the isotropic feature of the cube-like structure of NPs. The obtained nPEG-$TiO_2$ NPs nanostructured surface was then used to immobilize proteins (anti-rIgG,) and to

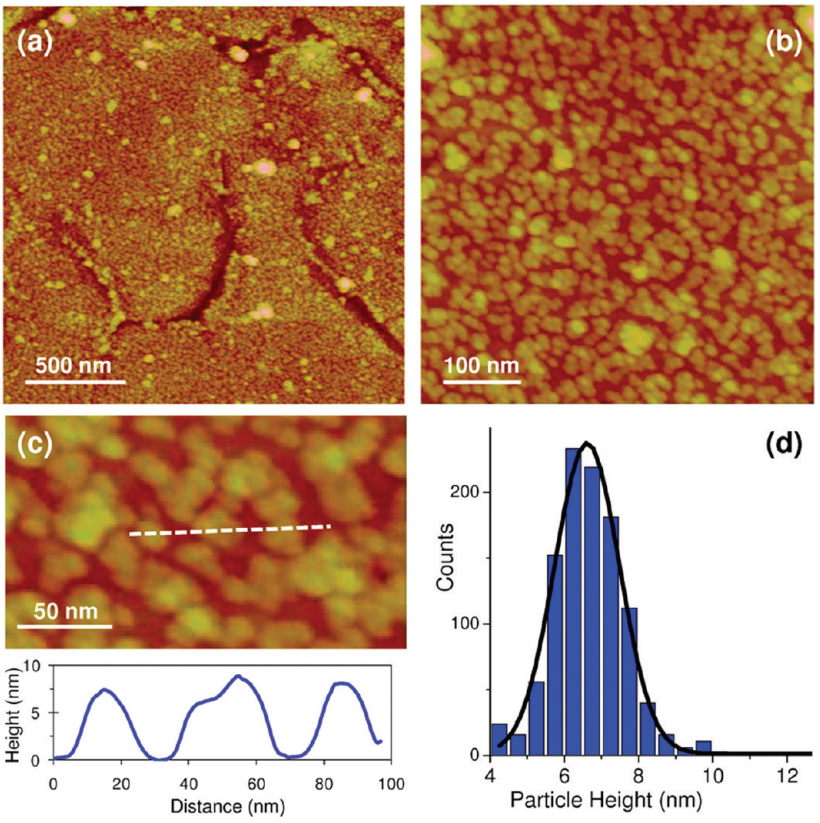


**Figure 3.** (a, b) AFM height images (Peak Force Tapping mode, in air; *z* scale 50 nm) of nPEG-$TiO_2$ nanoparticles immobilized on a cysteamine terminated gold surface. (c) Cross-sections were taken along the dashed line. (d) Histogram of the nanoparticle heights.

examine the efficiency of specific target recognition (rIgGs). The strategy to surface chemical modification is depicted in Scheme 2. The effect of PEG chains, regarding non specific protein adsorption, was checked using BSA. This procedure was fully characterized using PM-IRRAS analyses performed on the Au surface (Figure 2, Panel B). Starting from anti-rIgG deposition, the appearance of very intense amide bands at 1650 and 1550 $cm^{-1}$, can be noticed, suggesting a successful immobilization of the anti-rIgG. When this protein-terminated layer was exposed to BSA adsorption, its spectroscopic signature was unchanged (Figure 2, panel B: amide band area equal to 12.6 and 12.8 a.u for anti-rIgG and BSA, respectively), indicating that no significant amount of BSA molecules was adsorbed on the sensing layer. This result proves the successful role of PEG functions in avoiding non specific interactions. Eventually, the interaction with a rIgG solution led to a considerable increase of amide band area (Figure 2, panel B) evidencing the efficient recognition of the target by the biosensing layer. The integrated amide band area was 17.2 a.u., indicating a rather low but reasonable anti-rIgG/rIgG ratio close to 0.5, considering the strong repulsive effect of PEG chains.

## CONCLUSION

A new one-step solvothermal method was successfully applied to synthesize dicarboxylic acid-terminated PEG cubic $TiO_2$ nanocrystals. The latter displays terminal acid functions that allowed their immobilization on a cysteamine-terminated gold surface, leaving available acid functions for further protein attachment. The immobilization on flat gold substrates led to nanostructured surfaces of well dispersed $TiO_2$ nanoparticles. These platforms were used to build up a model biosensor and test its reactivity and selectivity for a model antigen/antibody. Immobilized antibodies were able to recognize antigens with a good specificity, likely due to the presence of PEG chains. This successful procedure provides a simple way to create nanostructured functional surfaces that favor good dispersion and accessibility of proteins. Our results open up a new route towards the elaboration of controlled and efficient nanostructured sensing surfaces.

## AUTHOR INFORMATION

### Corresponding Author

*E-mail: claire-marie.pradier@upmc.fr. Tel: +33 1 44 27 55 33. Fax: +33 1 44 27 60 33.

## REFERENCES

(1) Van der Molen, R.; Hurks, H.; Luiting, C. O.; Spies, F.; Van't Noordende, J.; Koerten, H.; Mommas, A. *Photochem. Photobiol.* **1998**, *J. B44*, 143.

(2) Caricato, A. P.; Manera, M. G.; Martino, M.; Rella, R.; Romano, F.; Spadavecchia, J.; Tunno, T.; Valerini, D. *Appl. Surf. Sci.* **2007**, *19*, 7937.

(3) Melcarne, G.; De Marco, L.; Carlino, E.; Martina, F.; Manca, M.; Cingolani, R.; Gigli, G.; Ciccarella, G. *J. Mater. Chem.* **2010**, *20*, 7248.

(4) De Marco, L.; Manca, M.; Giannuzzi, G.; Malara, F.; Melcarne, G.; Ciccarella, G.; Zama, I.; Cingolani, R.; Gigli, G. *J. Phys. Chem. C* **2010**, *114*, 4228.

(5) Mckenzie, K. J.; Marken, F. M. O. *Bioelectrochemistry* **2005**, *66*, 41.

(6) Topoglidis, E.; Campbell, J. C.; Cass, A. E. G.; Durrant, J. R. *Langmuir* **2001**, *17*, 7899.
(7) Topoglidis, E.; Cass, A. E. G.; Gilardi, G.; Sadeghi, S.; Beaumont, N.; Campbell; Cass, A. E. G.; Durrant, J. R. *Anal.Chem.* **1998**, *70*, 5111.
(8) Zhang, Y.; PL, H. E.; Hu, N. F. *Electrochim. Acta* **2004**, *49*, 1981.
(9) Wu, C. I.; Huang, J. W.; Wen, Y. L.; Wen, S.-Bi.; Shen, Y. H.; Yeh, M. Y. *Mater. Lett.* **2008**, *62*, 1923.
(10) Daimei, C.; Zhongyi, J.; Jiaquing, G.; Juhang, Z.; Dong, Y. *J. Nanoparticle Res.* **2008**, *2*, 303.
(11) Liao, D. L.; Wu, G. S.; Liao, B. Q. *Colloids Surf., A* **2009**, *348*, 270.
(12) Ciccarella, G.; Cingolani, R.; De Marco, L.; Gigli, G.; Melcarne, G.; Martina, F.; Matteucci, F.; Spadavecchia, J. World Patent 2009/101640.
(13) Parra, R.; Goès, M. S.; Castro, M. S.; Longo, E.; Bueno, P. R.; Varela, J. A. *Chem. Mater.* **2008**, *151*, 1653.
(14) Termnak, S.; Triampo, W.; Triampo, D. J. *Ceramic Process Res.* **2009**, *10*, 491.
(15) ManLee, L.; Heimork, R. L.; Baygents, J. C.; Zohar, Y. *Nanotechnology* **2006**, *17*, 529.
(16) Pinna, N.; Garnweitner, G.; Antonietti, M.; Niederberger, M. *Adv. Mater.* **2004**, *16*, 2197.
(17) Niederberger, M.; Pinna, N.; Polleux, J.; Antonietti, M. *Angew. Chem., Int. Ed.* **2004**, *43*, 2270.
(18) Jun, Y. W.; Casula, M. F.; Sim, J. H.; Kim, S. Y.; Cheon, J.; Alivisatos, A.P. *J. Am. Chem. Soc.* **2003**, *125*, 15981.
(19) Cozzoli, P. D.; Kornowski, A.; Weller, H. *J. Am. Chem. Soc.* **2003**, *125*, 14539.
(20) Niederberger, M.; Bartl, M. H.; Stucky, G. D. *Chem. Mater.* **2002**, *14*, 4364.
(21) Spadavecchia, J.; Moreau, J.; Hottin, J.; Canva, M. *Sens. Actuators, B* **2009**, *143*, 139.